Deuterium NMR Investigation of Backbone Dynamics in the Synthetic Oligonucleotide [d(CGCGAATTCGCG)]$_2$†

Todd M. Alam,‡ John Orban,§ and Gary P. Drobny*
Department of Chemistry, BG-10, University of Washington, Seattle, Washington 98195
Received December 18, 1990; Revised Manuscript Received June 28, 1991

ABSTRACT: Backbone dynamics in the [5′,5″-$^2H_2$]2′-deoxythymidine labeled duplex dodecamer [d(CGCGAAT*T*CGCG)]$_2$ have been investigated by solid-state ^2H NMR. Quadrupolar echo line shapes, spin-lattice relaxation, and quadrupolar echo decay times were obtained over hydration levels ranging from $W = 0.0$ to 25.2 (moles of H_2O/mole of nucleotide). Variation of the line shape with changing hydration level was analyzed by using models employed in previous investigations of dodecamer base and sugar dynamics. Both fast local motions and a slower helix motion were present within the oligonucleotide. The fast motion was modeled as a four-site libration whose amplitude increased with hydration level. The root mean square amplitude of this librational model was 2–6° larger than the amplitude observed in either the furanose ring or base labeled material for the entire range of hydration levels investigated. The observed line shape was inconsistent with a rapid three-site trans–gauche isomerization. A slow motion about the helix axis was observed at low water levels and increased in rate and amplitude with hydration. This motional model is in agreement with previous oligonucleotide studies.

The static structure and dynamic properties of DNA may prove useful in understanding the mechanism of its biological function. There have been numerous investigations into the internal dynamics of polynucleotides in recent years, including a number of ^1H, ^{31}P, and ^{13}C high-resolution NMR relaxation studies of backbone and base dynamics (Bolton & James, 1979, 1980a,b; Hogan & Jardetzky, 1979, 1980; Opella et al., 1981). In many of these studies the relaxation was assumed to be dominanted by fast localized internal motions, with no significant contributions from collective deformations. For instance, a ^{31}P NMR relaxation study by Hogan and Jardetzky modeled the backbone dynamics in DNA as a simple two-state jump and concluded that all three P–H vectors (P–H5′, P–H5″, and P–H3′) fluctuate with an amplitude of ~±20° or a later revised value of ±27° (Hogan & Jardetzky, 1979, 1980). Allison et al. (1982) have evaluated the contribution of torsional deformational modes to the ^{31}P NMR relaxation in DNA and reexamined the data of Hogan and Jardetzky. Allowing contributions from collective torsional modes, the total root mean squared (rms) amplitude of motion was not significantly different than the amplitude reported for a two-state model, but the relaxation was dominated by collective torsional deformations, not local internal motions.

Characterization of internal dynamics in DNA has typically involved fragments consisting of 100 base pairs or more. Unfortunately the relaxation mechanisms for longer DNA fragments can be quite complex. The relative contributions of collective torsional and bending motions versus local conformational fluctuations are still not fully understood. Relaxation in shorter DNA fragments is expected to have smaller contributions from collective motions, suggesting that investigation of synthetic oligonucleotides may allow separation of local fluctuations from collective dynamics. The solution study of oligonucleotides has received renewed interest with the improvement of synthetic protocols. Investigation of base dynamics in poly(dA-dT)·poly(dA-dT) (53 ± 15 base pairs) suggests that the angular displacement may be as large as ±32° (Assu-Munt et al., 1984). Similar studies of poly(dG-dC)·poly(dG-dC) (60 ± 10 base pairs) suggest a large out-of-plane motion of approximately 30–40° in the nanosecond range (Mirau et al., 1985). Recent studies on the synthetic oligonucleotides $[d(CG)_4]_2$ and $[d(CG)_6]_2$ using depolarized dynamic light scattering and NMR relaxation experiments modeled the internal base motion as diffusion in a cone with an amplitude of 29° or an over-damped libration of amplitude 18° (Eimer et al., 1990).

The use of the anisotropic spin interactions in solid-state NMR allows one to probe both the rate and amplitude of internal motions from analysis of line shapes and spin–lattice relaxation. Dynamics of the phosphate group in DNA fibers and powder samples have been studied by ^{31}P NMR (Mai et al., 1983; Fujiwara & Shindo, 1985). These investigations attribute the averaging of the line shape to diffusion about the long helix axis or a superposition of local and collective motions with a total angular fluctuation of ±30°. There have also been numerous investigations of internal base dynamics in nucleic acids utilizing solid-state ^2H NMR (DiVerdi & Opella, 1981; Bendel et al., 1983; Vold et al., 1986; Brandes & Kearns, 1986; Brandes et al., 1988; Shindo et al., 1987).

In this paper, we report the first solid-state ^2H NMR investigation of backbone dynamics in DNA. The variation in quadrupolar echo line shape, spin-lattice relaxation $\langle T_1 \rangle$, and quadrupolar echo decay times $\langle T_{2e} \rangle$ as a function of hydration for the [5′,5″-$^2H_2$]2′-deoxythymidine labeled dodecamer [d(CGCGAAT*T*CGCG)]$_2$ allows the development of a motional model to describe the dynamics of the sugar backbone. This self-complementary dodecamer contains the *Eco*RI endonuclease restriction site and has been the focus of numerous solution and solid-state investigations. For instance, this sequence was the first oligonucleotide single crystal investigated containing a complete turn of double-helical B-form DNA (Wing et al., 1980) and has been the subject of several

† This work was supported by a NIH program project Grant (GM 32681-07) and a NIH Molecular Biophysics Grant to T.M.A. (GM 08268-02).
‡ Present address: Department of Chemistry, University of Arizona, Tucson, AZ 85721.
§ Present address: Center for Advanced Research in Biotechnology (CARB), University of Maryland, 9600 Gudelsky Drive, Rockville, MD 20850.

0006-2960/91/0430-9229$02.50/0

X-ray diffraction investigations (Dickerson & Drew, 1981; Kopka et al., 1985; Pjura et al., 1987). In addition, information on the dynamics and local mobility within the dodecamer crystal has been obtained from a rigid segment analysis (Holbrook & Kim, 1984).

The sequence has also been investigated by using high-resolution 2D NMR, from which a distance geometry solution structure has been obtained (Nerdal et al., 1989). Solid-state ^{2}H NMR has been used to study the internal dynamics of the bases (Kintanar et al., 1989), the methyl groups of dT7 and dT8 (Alam & Drobny, 1990a,b), and the furanose rings of dA5 and dA6 in the dodecanucleotide (Huang et al., 1990). In this paper, these solid-state ^{2}H NMR investigations are extended to include the dynamics of the 5′,5″-deuterons of dT7 and dT8, allowing a comparison of motions between different regions of the double helix. The Theoretical Background section gives a brief review of solid-state ^{2}H NMR and the effects of motion on the observed line shape. The supplementary material presents an improved synthetic protocol for the incorporation of the deuterium label into the backbone. The Results section presents a solid-state ^{2}H NMR study of the [5′,5″-$^2H_2$]2′-deoxythymidine monomer and provides a basis for the remaining sections, which develop and evaluate different backbone motional models for the labeled dodecamer.

Theoretical Background

To understand the line-shape analysis, a brief review of solid-state ^{2}H NMR is presented. For an isolated deuteron in a solid, the NMR frequency is given by

$$\omega = \omega_0 \pm \omega_Q \tag{1}$$

The angular dependent quadrupolar frequency is given by

$$\omega_Q = 3\pi/4(e^2qQ/h)(3\cos^2\Theta - 1 + \eta\sin^2\Theta\cos 2\Phi) \tag{2}$$

where (e^2qQ/h) is the quadrupolar coupling constant (QCC) and η is the asymmetry parameter describing deviation from cylindrical symmetry of the electrical field gradient (EFG) tensor about the q_{zz} axis in the principal axis system (PAS). The polar angles Θ and Φ describe the orientation of the magnetic field $\mathbf{B}_0$ in the PAS of the EFG tensor. In general the diagonal elements of the EFG tensor are defined $|V_{xx}| \leq |V_{yy}| \leq |V_{zz}|$ and $\eta = (V_{xx} - V_{yy})/V_{zz}$ such that $0 \leq \eta \leq 1$ (Abragam, 1961).

Internal dynamics and molecular motion can modulate the quadrupolar frequencies, producing changes in the line shape. If the motion is slow on the time scale of ω_Q^{-1}, the observable effects on the quadrupolar echo line shape are minimal. Spectra in this limit are usually referred to as static line shapes and allow the determination of QCC_{static} and η_{static}. If the motion occurs within the intermediate exchange region ($\sim \omega_Q^{-1}$), it becomes necessary to simulate the modulation effect of these molecular motions on the quadrupolar frequencies. For short pulses, use of exchange-modified Bloch equations allows the line shapes to be determined for various motional models. The equation of motion for the complex transverse magnetization vector is given by

$$d\sigma_\pm/dt = [i\Omega_\pm + R]\sigma_\pm \tag{3}$$

where $\sigma_\pm$ corresponds to the single transition raising operators $[I_x(12) + iI_y(12)]$ or $[I_x(23) + iI_y(23)]$. The indices i,j in $I_{xy}(ij)$ label the eigenstates of the isolated deuteron where $|-1\rangle = |1\rangle, |0\rangle = |2\rangle$ and $|+1\rangle = |3\rangle$. The frequency domain spectra for the transitions are mirror images, requiring calculation of only one transition. The term $\Omega_\pm$ is a diagonal matrix containing the Larmor precession frequencies ω_Q, while the exchange operator R can be represented by $R = D\nabla^2$ for diffusion or a jump kinetic matrix R_{ij} for discrete motions. All quadrupolar echo line-shape simulations in this paper employ the discrete jump kinetic matrix approach, which has been discussed in detail elsewhere (Greenfield et al., 1987; Wittebort et al., 1987). If the molecular motion is fast on the time scale of ω_Q^{-1}, the line shape is defined by using QCC_{eff} and η_{eff}, the effective coupling constant and the effective asymmetry parameter of the averaged electrical field gradient tensor, such that the resonant frequency is given by

$$\omega_Q = 3\pi/4(e^2qQ/h)_{eff}[3\cos^2\Theta - 1 + \eta_{eff}\sin^2\Theta\cos 2\Phi] \tag{4}$$

Analysis of different models to describe rapid exchange will involve comparison of QCC_{eff} and η_{eff} with experimental values. The formalism for this correlation time-dependent analysis has been described previously (Wittebort et al., 1987). Expressions for three specific discrete motional models are developed in the Appendix.

Experimental Procedures

Solid-State NMR Spectroscopy. Solid-state ^{2}H NMR spectra were obtained at 76.75 MHz with quadrature phase detection and a μVaxII controlled home-built spectrometer. An eight-step phase-cycled quadrupolar echo sequence, $\pi/2_x$–τ_1–$\pi/2_{\pm y}$–τ_2–acq, was used with $\pi/2$ pulses less than 3 μs (Griffin, 1981). The pulse spacing τ_1 was varied from 50 to 200 μs, with the data acquisition being initiated prior to the echo by adjustment of τ_2. The recycle delay was at least 5 times T_1. The time domain signal was left-shifted prior to Fourier transformation. Lorentzian line broadening of 1500–3000 Hz was applied to experimental spectra to obtain an adequate signal-to-noise ratio.

Deuterium spin–lattice relaxation times were obtained by using an inversion–recovery pulse sequence. The magnetization recovery was determined from the quadrupolar echo height maximum, commonly referred to as a "powder average" and denoted as $\langle T_1 \rangle$. A nonlinear least-squares analysis (DeFontaine et al., 1975) was used to fit the magnetization recovery to the exponential

$$S(t) = S(\infty)[1 - 2e^{-t/T_1}] \tag{5}$$

The irreverible loss of phase memory as a function of pulse spacing, referred to as $\langle T_{2e} \rangle$, was also fit to an exponential recovery curve. Correlation times (τ_c) were calculated from the corresponding T_1 values according to the formalism presented by Torchia and Szabo (1982).

Line-Shape Simulations. Simulations of the ^{2}H NMR line shapes were obtained with the program MXQET, which can accommodate multisite, multiaxis motional models including corrections for finite pulse power, exchange during the pulse, and virtual FID effects. This program has been describe in extensive detail elsewhere (Greenfield et al., 1987). Effective values of the quadrupolar coupling constant (QCC_{eff}) and asymmetry parameter (η_{eff}) were determined from simulation of experimental line shapes, assuming no motional models.

Results

The solid-state ^{2}H NMR spectrum of [5′,5″-$^2H_2$]2′-deoxythymidine at 76.75 MHz is shown in Figure 1, along with a rigid-lattice simulation. This simulation yields the effective values of the quadrupolar coupling constant and asymmetry parameter, QCC_{eff} = 164 kHz and η_{eff} = 0.07. The spin–lattice relaxation recovery curve for the monomer was found to be highly nonexponential. The fast component relaxed with

Table I: Line-Shape Parameters and Relaxation Rates of [d(CGCGAAT*T*CGCG)]$_2$[a]

RH%	W[b]	RI[c]	QCC_{eff} (kHz)	η_{eff}	$\langle T_1 \rangle$ (ms)	$\langle T_{2e} \rangle$ (μs)
dry	0.0	1.00	164 ± 1	0.06	505 ± 51	165 ± 17
66	4.8	0.94	164 ± 1	0.06	206 ± 21	123 ± 12
75	10.5	0.18	152 ± 2	0.06	59 ± 10	125 ± 24
80	11.9	0.28	150 ± 2	0.06	41 ± 10	130 ± 13
88	16.3	0.48	143 ± 2	0.00	40 ± 10	101 ± 10
90	20.5		143 ± 4			
92	25.2		~0[d]	~0[d]		

[a] T* refers to the labeled [5′,5″-$^2H_2$]2′-deoxythymidine. [b] Moles of H_2O/mole of nucleotide. [c] Relative echo intensity with respect to dry. [d] Observed only the isotropic component.

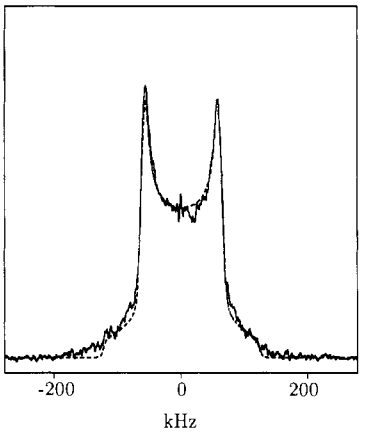

FIGURE 1: Experimental (—) and simulated (---) 76.75-MHz solid-state deuterium quadrupole echo spectra of [5′,5″-$^2H_2$]2′-deoxythymidine at 298 K. A 50-mg sample required 12 000 scans with a recycle time of 15 s to ensure thermal equilibrium. The $\pi/2$ pulse length was 2.3 μs, and the delay between pulses was 50 μs. The simulated spectrum was calculated by assuming a rigid-lattice model with QCC_{eff} = 164 kHz and η_{eff} = 0.07.

a $\langle T_1 \rangle$ of ~184 ms, while the slower component recovered with $\langle T_1 \rangle$ of ~1.18 s. The quadrupolar decay time $\langle T_{2e} \rangle$ for the [5′,5″-$^2H_2$]2′-deoxythymidine monomer was 150 μs.

Solid-state ^2H NMR spectra, spin–lattice relaxation times $\langle T_1 \rangle$, and quadrupolar echo decay times $\langle T_{2e} \rangle$ were obtained for [5′,5″-$^2H_2$]2′-deoxythymidine labeled [d(CGCGAAT*T*CGCG)]$_2$ as a function of relative humidity (RH) and water content W (moles of H_2O/mole of nucleotide) ranging from dry (W = 0.0) to 92% RH (W = 25.2). Effective quadrupolar coupling constants QCC_{eff}, effective asymmetry parameters η_{eff}, relative intensities (RI), $\langle T_1 \rangle$, and $\langle T_{2e} \rangle$ are presented in Table I. Representative line shapes as a function of hydration for the backbone labeled dodecamer are shown in Figure 2.

No significant changes in the line shape were observed for the increase in relative humidity from dry (W = 0.0) to 66% RH (W = 4.8, Figure 2A). There was a 12-kHz reduction of QCC_{eff} on hydrating to 75% RH (W = 10.5) plus an additional 2-kHz reduction on hydration to 80% RH (W = 11.9, Figure 2B). Between 80% RH (W = 11.9) and 88% RH (W = 16.3, Figure 2C), there was an additional 7-kHz reduction in QCC_{eff} resulting in the final value of 143 kHz. At 90% RH (W = 20.5, Figure 2D) the signal-to-noise ratio was reduced, with the spectrum being dominated by a central isotropic component, but a splitting corresponding to an approximate QCC_{eff} of 143 kHz was observed. At 92% RH (W = 25.2) only a central isotropic component was observed. Other line-shape characteristics included a nearly constant effective asymmetry parameter η_{eff} of ~0.06 through 80% RH (W = 11.9), along with a distinct loss of center intensity on increasing hydration from 66% RH (W = 4.8) through 88% RH (W = 16.3). A decrease of relative intensity with increasing water content was observed with the exception of 88% RH (W = 16.3) where the RI increased from that at 80% RH (W = 11.9). The variable behavior of $\langle T_{2e} \rangle$ with increasing water content is presented in Table I.

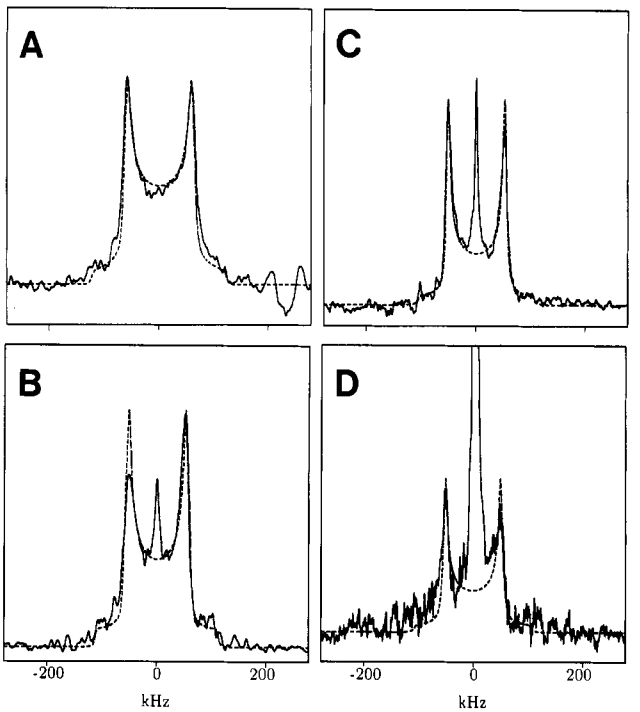

FIGURE 2: Experimental (—) and simulated (---) 76.75-MHz deuterium quadrupole echo spectra of [5′,5″-$^2H_2$]2′-deoxythymidine labeled [d(CGCGAATTCGCG)]$_2$ for various levels of water content W (moles of H_2O/mole of nucleotide). The simulated spectra were calculated as described in the text, ignoring the central isotropic component. With a pulse delay of 50 μs and $\pi/2$ pulse lengths varying from 2.3 to 3.0 μs, spectra were obtained for (A) 66% RH, W = 4.8, 60 000 scans, (B) 80% RH, W = 11.9, 116 750 scans, (C) 88% RH, W = 16.3, 144 000 scans, and (D) 90% RH, W = 20.5, 288 000 scans.

Spin–lattice relaxation recovery curves for the dodecamer were defined by a single exponential. For the dry (W = 0.0) dodecamer, the $\langle T_1 \rangle$ was 505 ms, half the value observed in the dry monomer. Increasing the relative humidity to 66% RH (W = 4.8) produced an additional 2-fold decrease in the relaxation time (Table I). The $\langle T_1 \rangle$ relaxation decreased by an additional factor of 4 on hydration to 75% RH (W = 10.5) and remained essentially unchanged (~40–50 ms) through 88% RH (W = 16.3). Spin–lattice relaxation and echo decay times were not determined for 90% RH (W = 20.5) and higher hydration levels due to the dominance of the isotropic peak.

Discussion

Internal Dynamics of the 5′-Methylene Group. The solid-state ^2H NMR spectrum of [5′,5″-$^2H_2$]2′-deoxythymidine has been reported previously (Kintanar et al., 1988). This investigation presents a superior synthetic protocol for preparation of the material, allowing increased sample size, purity, and improved signal-to-noise spectra. The effective values of

QCC_{eff} = 164 ± 1 kHz and η_{eff} = 0.07 ± 0.01 are slightly different than reported previously, but the line shape is still consistent with the absence of fast large-amplitude motions. The assumption of equivalent quadrupolar coupling constants for the 5′- and 5″-labeled positions has been addressed previously (Kintanar et al., 1988). The observed QCC was somewhat smaller than that reported for aliphatic systems (Rinne & Depireux, 1974), and the observation of a nonzero asymmetry parameter is also unexpected. If the observed asymmetry parameter is assumed to result entirely from motions (i.e., η_{static} =0, η_{eff} > 0), a model utilizing discrete jumps between two orientations with a half angle of θ_0 = ±12° and QCC_{static} of 175 ± 1 kHz gives the observed η_{eff}. This value of QCC_{static} is consistent with the value reported previously for the monomer (Kintanar et al., 1988) but is high in the range reported for other methylene groups (Rinne & Depireux, 1974). The question arises, How unique are the solutions for θ_0 and QCC_{static}? Inspection of eq A6 reveals that for small displacements there is only one solution for the amplitude θ_0 for an observed η_{eff}. The uniqueness of QCC_{static} is easily seen by rearrangement of eqs A6 and A7 to yield

$$QCC_{static} = (1 + \eta_{eff})QCC_{eff} \quad (6)$$

Within the frame work of a two-site jump and small displacements there is only one possible solution for QCC_{static} for an observed value of η_{eff} and QCC_{eff}. The value of QCC_{static} = 175 kHz will be utilized for all further motional analysis of backbone dynamics within the dodecamer. When the T_1 relaxation expressions for a two-site jump and a libration amplitude of 12° are used, the $\langle T_1 \rangle$ of 1.18 s corresponds to a correlation time of 15 ps or 0.1 μs, but the line shape is inconsistent with the larger correlation time. In the previous monomer investigation (Kintanar et al., 1988), the larger correlation time was chosen on the basis of a low center intensity in the observed spectrum. The increased signal-to-noise ratio of the present sample (see Figure 1) reveals this observation was incorrect.

Backbone Dynamics in Hydrated [*d*-(*CGCGAATTCGCG*)]$_2$. Analysis of variation in the solid-state ^{2}H NMR line shape provides insight into the internal dynamics of the backbone. These studies rely on comparison of simulated line shapes for a given model to experiment. Line-shape analysis can never prove a model represents what is physically occurring within the system, but it can help dismiss certain models. Model-free approaches have been used in the interpretation of NMR relaxation in macromolecules (Lipari & Szabo, 1982). This approach utilizes a generalized order parameter S and an effective correlation time τ_e to describe the rate of motion. While this approach has utility for motions in the extreme narrowing limit, the previous observation in hydrated oligonucleotide samples of highly anisotropic multiaxis motions, ranging from intermediate to fast exchange time scales, invalidates a model-free analysis for the present ^{2}H NMR investigation.

There are several aspects of the line shape that need to be addressed. One of the primary changes is the reduction in QCC_{eff}, coupled with the observation of a nearly constant η_{eff} with increasing hydration. In modeling the local dynamics of the backbone, the possibility of large conformational changes over a range of interconversion rates was considered. In methylene chain polymers a crankshaft motion is often used to describe the molecular motions, and a similar model was applied to the dodecamer, involving fluctuations of ψ between the backbone conformations gauche–gauche (+sc), gauche–trans (ap), and the trans–gauche (–sc) (Saenger, 1984) with unequal site probabilities. Conformational energy surfaces

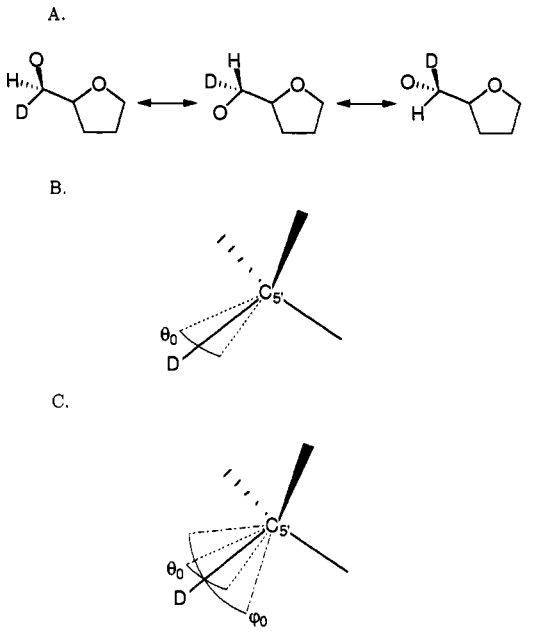

FIGURE 3: Figure of motional models. (A) Three-site trans–gauche isomerization, (B) a two-site libration with an amplitude defined by the half angle θ_0, and (C) a four-site libration with the amplitudes defined by the half-angles θ_0 and ϕ_0.

for 5′-nucleotides have been computed for rotation about the exocyclic C4′–C5′ bond. The +sc conformation corresponds to the global minimum while the energy of the ap and –sc conformations were found to be only 1 kcal/mol (Saran et al., 1972) or 2 and 1.3 kcal/mol, respectively (Yathindra & Sundaralingam, 1973) above the minimum. Yathindra and co-workers calculated the populations for the various conformations and reported values of 78% for +sc, 4% for ap, and 10% for –sc.[1] Line-shape simulations utilizing a discrete three-site trans–gauche isomerization with equilibrium site populations [$p_{eq}(i)$] of 85%, 5%, and 10% were initially investigated. The jump matrix R_{ij} used in these simulations must satisfy microreversibility, $k_{ij}p_{eq}(i) = k_{ji}p_{eq}(j)$, with k_{ii} being the negative sum of all rates depleting site i. The first model involves isomerization about the C4′–C5′ bond (see Figure 3A), which is the C_3 symmetry axis for the tetrahedral carbon. Variation of the line shape as a function of the jump rate k_{ij} is shown in Figure 4A. For large jump rates (fast exchange) the line shape undergoes significant averaging, leading to increased values of the effective asymmetry parameter (η_{eff} > 0.2), while at intermediate exchange rates distinct line shapes result, note particularly the disappearance of shoulder intensity. An extension of this motional model was to restrict the motion to a two-site isomerization. Simulations using unequal site populations [$p_{eq}(i)$] of 90% and 10% as a function of the jump rate k_{ij} are illustrated in Figure 4B. The differences between these simulations and experiment support the conclusion that large-amplitude trans–gauche interconversions between conformations of substantial equilibrium probability do not occur in the oligonucleotide backbone at

[1] The percent probability of occurrence for different conformations was determined with the expression

$$P(\chi,\psi) = 100 \times \exp[-V(\chi,\psi)/RT] / \sum_{\chi}\sum_{\psi} \exp[-V(\chi,\psi)/RT]$$

where $V(\chi,\psi)$ is the potential energy as a function of rotation about the C(1′)–N(9) (χ) and the C(4′)–C(5′) (ψ) bonds. The surface was calculated at 10° intervals of ψ and χ, resulting in percent totals less than 100% for the three discrete trans–gauche conformers used in the ^{2}H line-shape simulations.

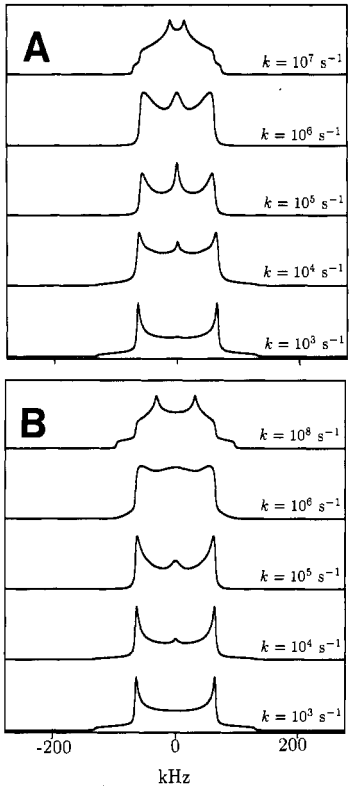

FIGURE 4: Simulations of backbone conformational conversions for a pulse delay of 50 μs as a function of jump rate k_{ij}. (A) Interconversion between gauche–gauche (+sc), gauche–trans (ap), and trans–gauche (–sc) with populations of 0.85 (site 1), 0.05 (site 2), and 0.10 (site 3), respectively. The site-to-site jump rates k_{12}, k_{13}, and $k_{2,3}$ were assumed to be equal. (B) Two-site diamond lattice jump with site population of 0.8 and 0.2 for differing jump rates k_{12}.

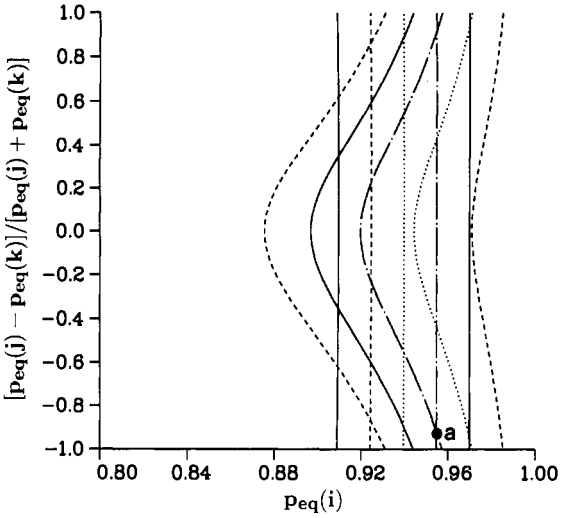

FIGURE 5: Variation in the effective asymmetry parameter η_{eff} and the reduction factor Λ for a three site jump as a function of the equilibrium population $p_{eq}(i)$ and the relative ratio of the remaining fractions $[p_{eq}(j)-p_{eq}(k)]/[p_{eq}(j) + p_{eq}(k)]$. Contours are shown for specific values of η_{eff}: 0.02 (- - -), 0.04 (···), 0.06 (—·—), 0.08 (—), 0.10 (- - -), and Λ (straight vertical contours); 0.96 (—), 0.94 (—·—), 0.92 (···), 0.90 (- - -), 0.88 (—). The solution ($\bullet_a$) corresponds to the dry and 66% RH line shapes, the remaining hydration levels have no possible solutions.

rates above $k_{ij} \sim 10^4$ s^{-1}. Figure 4A,B reveals the insensitivity of quadrupolar echo line shapes analysis to conformational changes occurring at rates slower that $\sim 10^3$ s^{-1}.

Information for the entire range of equilibrium populations in the fast exchange limit are easily obtained by using eq A9 for a three-site trans–gauche isomerization, to produce surfaces of the ratio $(e^2qQ/h)_{eff}/(e^2qQ/h)_{static}(\Lambda)$ and the effective asymmetry parameter η_{eff}. Figure 5 shows a contour plot of the overlap between these two surfaces as a function of the equilibrium population $p_{eq}(i)$ and the relative ratio the site populations between the two remaining sites. The region plotted is for the experimentally relevant range (η_{eff} = 0–0.08 and Λ = 1.0–0.82).

If QCC_{static} is assumed to be 175 kHz and η_{static} = 0, the line shape observed for the dry dodecamer corresponds to Λ ~ 0.94 and η_{eff} =0.06. Inspection of Figure 5 reveals that a rapid three-site trans–gauche isomerization with an equilibrium population of $p_{eq}(1)$ = 0.94, $p_{eq}(2)$ = 0.05, and $p_{eq}(3)$ = 0.01 (or equivalently $p_{eq}(2)$ = 0.01 and $p_{eq}(3)$ = 0.05) will produce these averaged line-shape parameters. The contour surface in Figure 5 also reveals the lack of possible solutions for averaged line shapes with η_{eff} = 0.06 and Λ < 0.89. Since the line shape observed at 75% RH (W = 10.5) corresponds to Λ = 0.87, a rapid three-site trans–gauche isomerization is unable to simulate this or higher hydration levels. The lack of a rapid trans–gauche isomerization within the backbone was not unexpected on the basis of previous molecular mechanics studies (Kollman et al., 1982) and molecular dynamics simulations (Levitt, 1983; Singh et al., 1985) in which the torsional angle ψ was found to be the least flexible. In the molecular dynamics simulations of the dodecamer [d(CGCGAATTCGCG)]$_2$ and other oligonucleotides, trans–gauche conformational changes were not observed except in terminal nucleotides. Small variations in the torsional angle were observed during the 80–90-ps simulations with rms fluctuations of 7° (Levitt, 1983) and 9–10° (Singh et al., 1985). A recent 100-ps molecular dynamics simulation of [d(CGCGAATTCGCG)]$_2$ contrasted to these earlier investigations with the observations of correlated trans–gauche isomerization at many different positions within the dodecamer (Srinivasan et al., 1990). These correlated motions may average the ^{2}H NMR line shape, but such effects were not observed. Due to the inability of this three-site trans–gauche isomerization model to explain the observed variation of the line shape with increasing hydration, except for the limiting case of the dry dodecamer, this motional model was not pursued further.

The variation in QCC_{eff} and η_{eff} has been simulated by various librational models in previous sugar and base investigations of the dodecamer. Since the static asymmetry parameter is assumed to be zero, the orientation of a librational plane with respect to a molecular or crystal frame is only possible from measurements on aligned samples. If the rate of internal libration is rapid, anisotropic librations can produce a nonzero effective asymmetry parameter η_{eff}. If additional motions occur within the sample (see later discussion) the orientation of these secondary motions can be described relative to the librationally averaged EFG tensor, but absolute orientation in a molecular or crystal frame will still require investigation of an aligned sample. While use of these models involves arbitrary orientations, consideration of the molecular or crystal environment may suggest preferred librational directions.

The simplest model considered is a two-site libration of the individual C–D bond (see Figure 3B). This model has been used to describe the base and methylene dynamics in the 2′-deoxythymidine monomer (Kintanar et al., 1988) and the sugar dynamics in 2′-deoxyadenosine (Huang et al., 1990) along with the base dynamics in the labeled dodecamer (Kintanar et al., 1989; Alam & Drobny, 1990a,b). Assuming QCC_{static} = 175 kHz and η_{static} =0.0, the reduction in QCC_{eff}

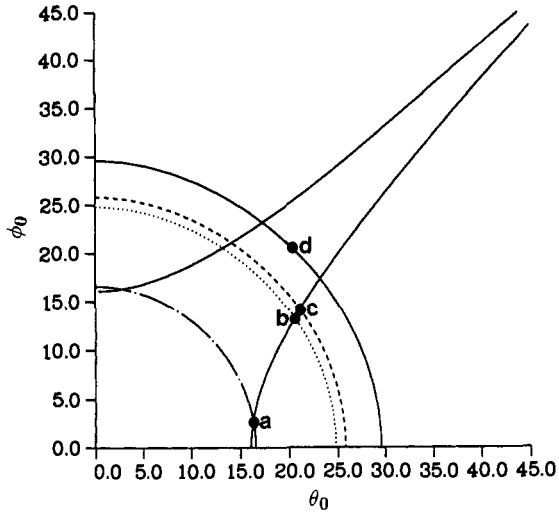

FIGURE 6: Variation in the effective asymmetry parameter η_{eff} and the reduction factor Λ for a four-site libration as a function of the half-angles θ_0 and ϕ_0. Contours are shown for specific values of η_{eff}; 0.06 (—), and Λ; 0.94 (—·—), 0.87 (···), 0.86 (- - -), 0.82 (—). Solutions for the different hydration levels are shown; dry and W = 4.8 ($\bullet_a$), W = 10.5 ($\bullet_b$), W = 11.9 ($\bullet_c$), W = 16.3, and W = 20.5 ($\bullet_d$). Note that solution ($\bullet_d$) is for η_{eff} = 0.0, which corresponds to the graph diagonal.

for dry (W = 0.0) and 66% RH (W = 4.8) can be accounted for by including a libration of $\theta_0 = 11.5 \pm 1°$ using eqs A6 and A7. The amplitude of this libration is similar to the rms fluctuations observed in the molecular dynamics simulations discussed above. When the relaxation expressions for a two-site libration are used, the $\langle T_1 \rangle$ of 505 ms for the dry (W = 0.0) dodecamer corresponds to a correlation time of 32 ps or 0.05 μs, while at 66% RH (W = 4.8) the $\langle T_1 \rangle$ of 206 ms corresponds to a correlation time of 85 ps or 0.02 μs. As observed in the monomer, the line shape is inconsistent with the longer correlation times. Attempts to extend this librational model to account for the 12-kHz reduction in QCC_{eff} upon hydration to 75% RH (W = 10.5) were unsuccessful. The large librational angle required to produce the motional averaging results in an increased effective asymmetry parameter η_{eff} (easily seen from inspection of eq A7), a trend not observed experimentally.

Another possible model to describe the internal dynamics in the DNA backbone is a biaxial four-site libration (see Figure 3C), consisting of displacement in two perpendicular planes (Brandes et al., 1988; Shindo et al., 1987; Kintanar et al., 1989; Alam & Drobny, 1990a). The biaxial model was defined by using θ_0 to describe librations parallel to the long helix axis of the dodecamer and ϕ_0 to describe librations in the plane perpendicular to the helix axis. The variation in QCC_{eff} and η_{eff} with increasing relative humidity can be explained by changes in θ_0 and ϕ_0 using eq A8 and is presented as a contour overlay in Figure 6. The value QCC_{static} = 175 kHz and η_{static} = 0.0 were used, and the line shape of the dry (W = 0.0) and 66% RH (W = 4.8) sample were simulated the $\theta_0 = 16 \pm 2°$ and $\phi_0 = 4 \pm 2°$. At 75% RH (W = 10.5) the librational angles increased to $\theta_0 = 20.5 \pm 4°$ and $\phi_0 = 13.5 \pm 4°$, while at 80% RH (W = 11.9) the angles were $\theta_0 = 22 \pm 4°$ and $\phi_0 = 15 \pm 4°$. At 88% RH (W = 16.3) $\theta_0 = 20.5 \pm 3°$ and $\phi_0 = 20.5 \pm 3°$, which remained unchanged for 90% RH (W = 20.5). It should be noted that in the line-shape analysis the angles were restricted to $\theta_0 \neq \phi_0$ to fulfill the requirement $\eta_{eff} \neq 0$. Inspection of Figure 6 reveals that for a given Λ and η_{eff} only symmetry-related solutions (i.e., amplitudes of θ_0 and ϕ_0 interchanged) are possible within the range investigated.

Table II: RMS Deviation of Biaxial Libration with Relative Humidity

	sample[a]				
RH%	A	B[b]	C[b]	D[b]	E
dry	8 ± 1°	5°		9°	12 ± 2°
66	8 ± 1°	7°	10°	10°	12 ± 2°
75	11 ± 2°				17 ± 4°
80	11 ± 2°	9°	12°	14°	19 ± 4°
88	18 ± 2°	5°		16°	21 ± 3°

[a] A = [*methyl*-^{2}H]2′-deoxythymidine, [d(CGCGAAT*T*CGCG)]$_2$; B = [H8-^{2}H]2′-purine, [d(CG*CG*A*A*TTCG*CG*)]$_2$; C = [H6-^{2}H]2′-deoxythymidine, [d(CGCGAAT*TCGCG)]$_2$; D = [2″-^{2}H]2′-deoxyadenosine, [d(CGCGA*A*TTCGCG)]$_2$; E = [5′,5″-$^2H_2$]2′-deoxythymidine, [d(CGCGAAT*T*CGCG)]$_2$. [b] Relative errors for libration angles were not reported for these samples but are assumed to be similar to the errors obtained for the methyl- and 5′,5″-labeled dodecamer.

It is interesting to compare the root mean square (rms) amplitude of the backbone deuterons obtained from this four-site libration model to the rms amplitude observed in previous ^{2}H NMR investigations of the dodecamer. The rms amplitude for the four-site jump is defined as

$$\mathrm{rms}(\theta_0,\phi_0) = \sqrt{\frac{\theta_0^2 + \phi_0^2}{2}} \qquad (7)$$

The results through 88% RH ($W \approx 15$) are shown in Table II. While the dynamic amplitude of the backbone deuterons is always greater than that observed for the base or sugar positions by 2–6°, it never greatly exceeds the amplitude of base and sugar libration at any hydration level. Rill et al. (1983) observed the effects of intermolecular interactions on internal dynamics in the ^{13}C NMR investigation of spontaneous ordering of DNA (147, 234, and 437 base pairs). At concentrations as low as 6.5 mg mL^{-1}, motions of the C5′ were slowed, while the dynamics of the C2′ remained rapid even in the oriented phase. The concentration of the [5′,5″-$^2H_2$]-2′-deoxythymidine labeled dodecamer sample hydrated at 90% RH (W = 25.5) was 940 mg mL^{-1}. Due to the high concentration levels present, intermolecular interactions may account for the similarity between the observed rms amplitude of the backbone dynamics and the rms amplitude of the base or sugar 2″.

Characterization of the local mobility in nucleic acids from crystallographic data using a segmented rigid body model found that the phosphate backbone has the largest rms amplitude in comparison to other groups of the nucleotide (Holbrook & Kim, 1984). The eignevector clusters for the librational matrix were determined for the dodecamer. The rms amplitudes of the phosphate librations[2] were found to be approximately 29° and 20°, while the librations of the ribose were 32° and 22° and the base librations were 14°, 17°, and 18°. The magnitude of these librations is significantly larger than those obtained from ^{2}H line-shape analysis using a four-site librational model. These differences may be model dependent or reflect conformational disorder and rigid body librational disorder within the crystal.

The rate of these fast internal librations cannot be determined from analysis of quadrupolar echo line shapes alone except for a lower limit on the rate. While the fast librations have been modeled as a four-site jump, the exact nature of the motion including the possibility of contributions from

[2] The orientation of the librational eigenvectors is discussed in Holbrook and Kim (1984).

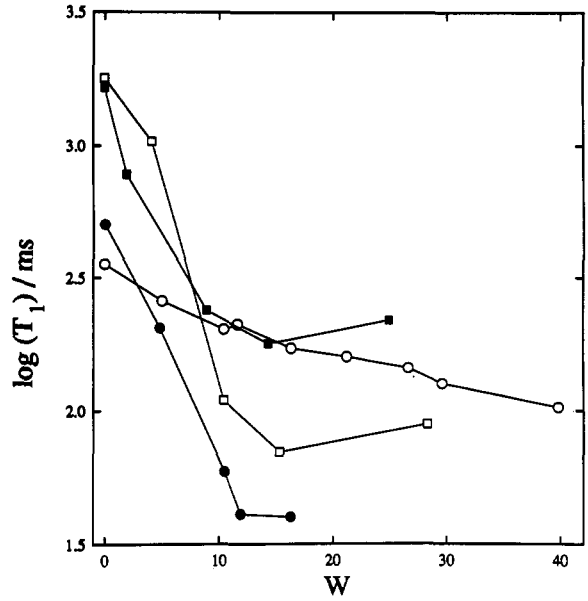

FIGURE 7: ^{2}H spin-lattice relaxation $\langle T_1 \rangle$ as a function of hydration level W (moles of H_2O/mole of nucleotide) for various labeled positions in the dodecamer. (●) [5′,5″-$^2H_2$]2′-deoxythymidine labeled [d-(CGCGAAT*T*CGCG)]$_2$, (■) [8-^{2}H]purine labeled [d-(CG*CG*A*A*TTCG*CG*)$_2$], (○) [*methyl*-^{2}H]2′-deoxythymidine labeled [d(CGCGAAT*T*CGCG)$_2$], and (□) [2″-^{2}H]2′-deoxyadenosine labeled [d(CGCGA*A*TTCGCG)]$_2$.

collective motions cannot be determined from analysis of line shapes. A detailed investigation of spin–lattice relaxation at various magnetic field strengths, along with separation of the various spectral densities, would allow this problem to be addressed. A recent study by Brandes et al. (1990), which determined the spectral densities $J_1(\omega_0)$ and $J_2(2\omega_0)$ for oriented purine base labeled calf thymus fibers, hints at the complexity of motions occurring in DNA. They found that the large value of the J_1/J_2 ratio ruled out the possibility that in-plane torsional motions were the dominant factor in the relaxation mechanism. It was also noted that at higher hydration levels such torsional motions may have increasing contributions. While such detailed analysis is not possible with the present [5′,5″-$^2H_2$]2′-deoxythymidine labeled dodecamer, comparison of trends in the spin–lattice relaxation for various positions of the nucleotide is possible. Brandes et al. (1986) noted that the ratio between the ^{31}P relaxation obtained by Mai et al. (1983) for the backbone, and the ^{2}H relaxation of the purine bases in calf thymus DNA was approximately constant through hydration levels of $W = 20$. Similar trends were noted by Huang et al. (1990) between the ^{2}H relaxation of the sugar 2″ and the purine base (Kintanar et al., 1989) within the dodecamer [d(CGCGAATTCGCG)]$_2$. These trends suggest that the backbone, sugar, and base motions are coupled. Similar comparisons can be made between all the ^{2}H-labeled sites of the dodecamer. Spin–lattice relaxation time as a function of hydration is shown in Figure 7. The variation in relaxation for the various positions is similar from 66% RH ($W = 4.8$) through 88% RH ($W = 16.3$) with the notable exception of the methyl-labeled position. This last observation is not surprising in that the relaxation of the methyl group is strongly influenced by the rapid (10–50 ps) motion about the C_3 symmetry axis. The trend in the relaxation of the remaining labeled positions suggests that, within the 12 base pair oligonucleotide, the motions of the backbone, the sugar 2″, and the purine bases are similar. Analysis of ^{31}P relaxation within the dodecamer is presently being pursued in our laboratory.

While the fast four-site biaxial libration model describes the reduction in QCC_{eff} and η_{eff}, it does not explain all the observed variations in the line shape. Only the dry ($W = 0.0$) experimental line shape was adequately simulated by using a fast librational model alone. The invariance of fast exchange line shapes to the quadrupole echo sequence pulse spacing is inconsistent with the observed spectra of the dodecamer sample at hydration levels above 66% RH ($W = 4.8$), which reveal a loss of center intensity with pulse spacing. Similar changes have been noted in previous investigations of ^{2}H-labeled dodecamers (Kintanar et al., 1989; Alam & Drobny, 1990a,b) and are characteristic of anisotropic motions in the slow and intermediate exchange regime.

The possibility of slow motion about the long helix axis in addition to fast four-site internal librations was the next model investigated. We have utilized a model of N site nearest neighbor jumps to portray restricted diffusion about the helix axis described by the equilibrium

$$S_1 \underset{k_{21}}{\overset{k_{12}}{\rightleftharpoons}} S_2 \underset{k_{32}}{\overset{k_{23}}{\rightleftharpoons}} \cdots \underset{k_{n,n-1}}{\overset{k_{n-1,n}}{\rightleftharpoons}} S_n \qquad (8)$$

where S_i represents the ith site and k_{ij} is the jump rate between sites i and j (Fujiwara & Shindo, 1985; Shindo et al., 1987; Kintanar et al., 1989; Alam & Drobny, 1990a). If equal site populations are assumed a global jump rate k can be used to define a diffusion coefficient

$$D_R = k\theta_{ij}^2/2 \qquad (9)$$

where θ_{ij} is the arc angle between successive sites. The effects of the number of sites N and the jump size θ_{ij} on the ^{2}H NMR line shape have been discussed previously (Wittebort et al., 1987; Alam & Drobny, 1990a). In the present investigation only a six-site jump model was used to simulate motion about the helix axis, primarily to reduce computational time.

To model the effects of helix rotation on the line shape of the [5′,5″-$^2H_2$]2′-deoxythymidine labeled dodecamer, the orientation of the EFG tensor with respect to the helix axis needs to be considered. Assuming model B-form DNA, the 5′ and 5″ C–D bond forms angles of approximately 38° and 71° to the helix axis. The orientation of the biaxial libration was defined with displacements parallel to the helix rotation axis being defined as θ_0. Different orientations of the biaxial librations produced effects on the simulated line shape that were small compared to the detail obtainable from the low signal-to-noise ratio samples. The line shape at 66% RH ($W = 4.8$) was simulated by including a slow six-site helix axis motion at $k = 1$ kHz, $\theta_{ij} = 5°$, corresponding to $D_R = 3.8$ s^{-1} (Figure 2A). At 75% RH ($W = 10.4$) and 80% RH ($W = 11.9$) this helix motion increased to $k = 6$ kHz, $\theta_{ij} = 5°$, and $D_R = 22.8$ s^{-1} (Figure 2B). At 88% ($W = 16.3$) the simulation yields $k = 10$ kHz, $\theta_{ij} = 20°$, and $D_R = 609$ s^{-1} (Figure 2C). Even though the signal-to-noise ratio is highly reduced, the line shape at 90% RH ($W = 20.5$) is consistent with $k = 100$ kHz, $\theta_{ij} = 20°$, and $D_R = 6092$ s^{-1} (Figure 2D).

The values for the rate and amplitude of helix motion were quite similar to those observed in previous sugar and base investigations of the dodecamer through 88% RH ($W = 16.3$). The fact that for hydration levels through $W \approx 20$ the model of fast librations combined with a slow helix motion can explain the observed line shapes for all ^{2}H-labeled dodecamers examined to date suggests that it is indeed a reasonable, while perhaps not unique, model of dynamics in hydrated oligonucleotides.

The high hydration level of 90% RH ($W = 20.5$) could not be simulated with the values ($k = 400$ kHz, $\theta_{ij} = 60°$) obtained for the methyl-labeled dodecamer at 90% RH ($W = 21.2$),

since these values produced a line shape with greater motional averaging than observed experimentally. This hydration level was not investigated for either the sugar-labeled dodecamer (Huang et al., 1990), or the base-labeled dodecamer (Kintanar et al., 1989). In the investigation of the methyl- and 2″-labeled dodecamer at hydration levels of $W > 20$, contributions from diffusion about an axis perpendicular to the long helix axis were also employed to explain finer aspects of the experimental data. The poor signal-to-noise ratio observed for the [5′,5″-$^2H_2$]2′-deoxythymidine labeled dodecamer does not warrant such a detailed analysis and was not considered further. This inability to obtain rates that are consistent for the methyl- and backbone-labeled dodecamer at 90% RH may reflect subtle differences between the samples (i.e., hydration levels) or a weakness of the simplistic six-site jump to describe helix diffusion at higher hydrations.

Conclusions

In summary, the variation of the ^2H NMR spectra for the [5′,5″-$^2H_2$]2′-deoxythymidine labeled dodecamer [d-(CGCGAAT*T*CGCG)]$_2$ was studied as a function of hydration level. With higher hydration levels there is a steady increase in the librational amplitude modeled by using a four-site jump model. The rms amplitude of this libration was only slightly larger than the motional amplitude observed in the sugar 2″- or base-labeled investigations. A quantitative comparison of the base, sugar, and backbone relaxation revealed similar trends as a function of hydration, suggesting a similarity in the internal motions. At higher hydration levels, slow motion about the helix axis must be included to account for the observed experimental line shapes and is consistent with previous ^2H NMR studies involving the internal dynamics in synthetic oligonucleotides. Investigations of the phosphorus backbone using ^{31}P NMR as a function of hydration and oligonucleotide length are presently being pursued. Further investigations involving [2″-^2H]2′-deoxycytidine and labeled oligonucleotides are in progress.

Acknowledgments

We thank Dr. Paul Ellis, Dr. Regitze Vold, and Dr. Robert Vold for providing original copies of the simulation program MXQET. We also thank Dr. Paul Hopkins for the generous gift of 2-cyanoethyl-*N*,*N*,*N*′,*N*′-tetraisopropylphosphorodiamidite.

Appendix

Fast Exchange. If the motion is rapid on comparison to ω_Q^{-1}, the eigenvalues of the motionally averaged or quasistatic EFG tensor $\bar{V}_{ll}^{PAS}$ replace the principal components of the static V_{ll}^{PAS}. The equilibrium distribution $P(\Omega)$ determines the weighting for motionally averaging of the EFG tensor. For the discrete processes considered here (Wittebort et al., 1987)

$$\bar{V}_{kl} = \sum_j P(\Omega_j) V_{kl}(\Omega_j) \tag{A1}$$

Expressions for the EFG tensor at a given site j are obtained by using the orthogonal transformation

$$\mathbf{V}(\Omega_j) = \mathbf{r}^{\dagger}(\Omega_j)\mathbf{V}^{PAS}\mathbf{r}(\Omega_j) \tag{A2}$$

If the EFG tensor is axially symmetric ($\eta_{static} = 0$), it is described in the PAS by

$$\mathbf{V}^{PAS} = -\frac{eq}{2}\begin{pmatrix} 1 & 0 & 0 \\ 0 & 1 & 0 \\ 0 & 0 & -2 \end{pmatrix} \tag{A3}$$

requiring only two Euler angles $\Omega_j = (\theta_j,\phi_j)$ in the transformation to describe $\mathbf{V}(\Omega_j)$.

$$\mathbf{V}(\Omega_j) = -\frac{eq}{2} \times \begin{pmatrix} 1-3\cos^2\phi_j \sin^2\theta_j & 3/2 \sin 2\phi_j \sin^2\theta_j & 3/2 \cos\phi_j \sin 2\theta_j \\ 3/2 \sin 2\phi_j \sin^2\theta_j & 1-3\sin^2\phi_j \sin^2\theta_j & -3/2 \sin\phi_j \sin 2\theta_j \\ 3/2 \cos\phi_j \sin 2\theta_j & -3/2 \sin\phi_j \sin 2\theta_j & 1-3\cos\theta_j \end{pmatrix} \tag{A4}$$

The averaged EFG tensor resulting from a two-site libration or a two-site flip with a half angle of θ_0 is obtained by using eqs A1 and A4 and is given by

$$\bar{\mathbf{V}} = -\frac{eq}{2}\begin{pmatrix} 1-3\sin^2\theta_0 & 0 & \xi_{12}^{-}(3/2)\sin 2\theta_0 \\ 0 & 1 & 0 \\ \xi_{12}^{-}(3/2 \sin 2\theta_0 & 0 & 1-3\cos^2\theta_0 \end{pmatrix} \tag{A5}$$

where the sum or difference of equilbrium site populations is defined as $\xi_{ij}^{\pm} = [p_{eq}(i) \pm p_{eq}(j)]$. With diagonalization of the matrix shown in eq A5 and use of the definition $|V_{xx}| \leq |V_{yy}| \leq |V_{zz}|$ and $\eta = (V_{xx} - V_{yy})/V_{zz}$, expressions for a two-site libration are easily obtained and are similar to expressions previously reported (Pratum & Klein, 1989). For small angles of libration, $0° < \theta_0 < 35.3°$, the reduction in the effective quadrupolar coupling constant and the effective asymmetry parameter are given by

$$\Lambda = (e^2qQ/h)_{eff}/(e^2qQ/h)_{static} = P_2(\cos\theta_0) \tag{A6}$$

$$\eta_{eff} = [1 - P_2(\cos\theta_0)]/P_2(\cos\theta_0) \tag{A7}$$

where the ratio of the averaged over the static coupling constants are denoted as Λ. Expressions for a four-site libration with displacement in two perpendicular planes were obtained in a similar manner. For displacements of $\pm\theta_0$ (sites 1 and 2) and $\pm\phi_0$ (sites 3 and 4) the averaged EFG tensor is

$$\bar{\mathbf{V}} = -\frac{eq}{2} \times \begin{pmatrix} \xi_{34}^{+} + \xi_{12}^{+}(1-3\sin^2\theta_0) & 0 & \xi_{12}^{-}(3/2)\sin\theta_0 \\ 0 & \xi_{12}^{+} + \xi_{34}^{+}(1-3\sin^2\phi_0) & -\xi_{34}^{-}(3/2)\sin 2\phi_0 \\ \xi_{12}^{-}(3/2)\sin 2\theta_0 & -\xi_{34}^{-}(3/2)\sin 2\phi_0 & \xi_{12}^{+}(1-3\cos^2\theta_0) + \xi_{34}^{+}(1-3\cos^2\phi_0) \end{pmatrix} \tag{A8}$$

Diagonalization of this matrix allows determination of QCC_{eff} and η_{eff} for a given range of θ_0 and ϕ_0. A contour of solutions of Λ and η_{eff} is presented in Figure 6.

A three-site trans–gauche isomerization defined by the angles $\phi_1 = 0°$, $\phi_2 = 120°$, $\phi_3 = 240°$, and θ and the populations $p_{eq}(1) = 1 - \xi_{23}^{+}$ results in the averaged EFG tensor

$$\bar{\mathbf{V}} = -\frac{eq}{2} \times \begin{pmatrix} Peq(1)(1-3\sin^2\theta) + \xi_{23}^{+}(1-3/4\sin^2\theta) & -\xi_{23}^{-}(3\sqrt{3}/4)\sin^2\theta & Peq(1)(3/2)\sin 2\theta - \xi_{23}^{+}(3/4)\sin 2\theta \\ -\xi_{23}^{-}(3\sqrt{3}/4)\sin^2\theta & Peq(1) + \xi_{23}^{+}(1-(9/4)\sin^2\theta) & -\xi_{23}^{-}(3\sqrt{3}/4)\sin 2\theta \\ Peq(1)(3/2)\sin 2\theta - \xi_{23}^{+}(3/4)\sin 2\theta & -\xi_{23}^{-}(3\sqrt{3}/4)\sin 2\theta & 1-3\cos^2\theta \end{pmatrix} \tag{A9}$$

A contour plot for solutions of Λ and η_{eff} is presented in Figure 5.

Supplementary Material Available

A description of the procedures used in the synthesis of ^{2}H-labeled deoxythymidine derivatives and in the synthesis and purification of the DNA dodecamer (2 pages). Ordering information is given on any current masthead page.

Registry No. d(CGCGAATTCGCG)$_2$, 77889-82-8.

References

Abragam, A. (1961) in *Principles of Nuclear Magnetism*, pp 261–263, Oxford University Press, New York.

Alam, T. M., & Drobny, G. (1990a) *Biochemistry 29*, 3421–3430.

Alam, T. M., & Drobny, G. (1990b) *J. Chem. Phys. 92*, 6840–6846.

Allison, S. A., Shibata, J. H., Wilcoxon, J., & Schurr, J. M. (1982) *Biopolymers 21*, 729–762.

Assa-Munt, N., Granot, J., Behling, R. W., & Kearns, D. R. (1984) *Biochemistry 23*, 944–955.

Bendel, P., Boesch, J., & James, T. L. (1983) *Biochim. Biophys. Acta 759*, 205–213.

Bolton, P. H., & James, T. L. (1979) *J. Chem. Phys. 83*, 3359–3366.

Bolton, P. H., & James, T. L. (1980a) *Biochemistry 19*, 1388–1392.

Bolton, P. H., & James, T. L. (1980b) *J. Am. Chem. Soc. 102*, 25–31.

Brandes, R., & Kearns, D. R. (1986) *Biochemistry 25*, 5890–5895.

Brandes, R., Vold, R. R., Vold, R. L., & Kearns, D. R. (1986) *Biochemistry 25*, 7744–7751.

Brandes, R., Vold, R. R., & Kearns, D. R. (1988) *J. Mol. Biol. 202*, 321–332.

Brandes, R., Vold, R. R., Kearns, D. R., & Rupprecht, A. (1990) *Biochemistry 29*, 1717–1721.

DeFontaine, D. L., Ross, D. K., & Ternai, B. (1975) *J. Magn. Reson. 18*, 276–281.

Dickerson, R. E., & Drew, H. R. (1981) *J. Mol. Biol. 149*, 761–786.

DiVerdi, J. A., & Opella, S. J. (1981) *J. Mol. Biol. 149*, 307–311.

Eimer, W., Williamson, J. R., Boxer, S. G., & Pecora, R. (1990) *Biochemistry 29*, 799–811.

Fujiwara, T., & Shindo, H. (1985) *Biochemistry 24*, 896–902.

Greenfield, M. S., Ronemus, A. D., Vold, R. L., & Vold, R. R. (1987) *J. Magn. Reson. 72*, 89–107.

Griffin, R. G. (1981) *Methods Enzymol. 72*, 108–174.

Hogan, M. E., & Jardetzky, O. (1979) *Proc. Natl. Acad. Sci. U.S.A. 76*, 6341–6345.

Hogan, M. E., & Jardetzky, O. (1980) *Biochemistry 19*, 3460–3468.

Holbrook, S. R., & Kim, S.-H. (1984) *J. Mol. Biol. 173*, 361–388.

Huang, W.-C., Orban, J., Kintanar, A., Reid, B. R., & Drobny, G. P. (1990) *J. Am. Chem. Soc. 112*, 9059–9068.

Kintanar, A., Alam, T. M., Huang, W.-C., Schindele, D. C., Wemmer, D. E., & Drobny, G. (1988) *J. Am. Chem. Soc. 110*, 6367–6372.

Kintanar, A., Huang, W.-C., Schindele, D. C., Wemmer, D. E., & Drobny, G. (1989) *Biochemistry 28*, 282–293.

Kollman, P., Keepers, J. W., & Weiner, P. (1982) *Biopolymers 21*, 2345–2376.

Kopka, M. L., Yoon, C., Goodsell, D., Pjura, P., & Dickerson, R. E. (1985) *J. Mol. Biol. 183*, 553–563.

Levitt, M. (1983) *Cold Spring Harbor Symp. Quant. Biol. 47*, 251–275.

Lipari, G., & Szabo, A. (1982) *J. Am. Chem. Soc. 104*, 4546–4559.

Mai, M. T., Wemmer, D. E., & Jardetzky, O. (1983) *J. Am. Chem. Soc. 105*, 7149–7152.

Mirau, P. A., Behling, R. W., & Kearns, D. R. (1985) *Biochemistry 24*, 6200–6211.

Nerdal, W., Hare, D. R., & Reid, B. R. (1989) *Biochemistry 28*, 10008–10021.

Opella, S. J., Wise, W. B., & DiVerdi, J. A. (1981) *Biochemistry 20*, 284–290.

Pjura, P. E., Grzeskowiak, K., & Dickerson, R. E. (1987) *J. Mol. Biol. 197*, 257–271.

Pratum, T. K., & Klein, M. P. (1989) *J. Magn. Reson. 81*, 350–370.

Rill, R. L., Hilliard, P. R., & Levy, G. C. (1983) *J. Biol. Chem. 258*, 250–256.

Rinne, M., & Depireux, J. (1974) in *Advances in Nuclear Quadrupole Resonance* (Smith, J. A. S., Ed.) Vol. 1, pp 357–389, Pergamon, New York.

Saenger, W. (1984) in *Principles of Nucleic Acid Structure*, pp 23–24, Springer-Verlag, New York.

Saran, A., Pullman, B., & Perahia, D. (1972) *Biochim. Biophys. Acta 287*, 211–231.

Shindo, H., Hiyama, Y., Roy, S., Cohen, J. S., & Torchia, D. A. (1987) *Bull. Chem. Soc. Jpn. 60*, 1631–1640.

Singh, U. C., Weiner, S. J., & Kollman, P. (1985) *Proc. Natl. Acad. Sci. U.S.A. 82*, 755–759.

Srinivasan, J., Withka, J. M., & Beveridge, D. L. (1990) *Biophys. J. 58*, 533–547.

Torchia, D. A., & Szabo, A. (1982) *J. Magn. Reson. 49*, 107–121.

Vold, R. R., Brandes, R., Tsang, P., Kearns, D. R., & Vold, R. L. (1986) *J. Am. Chem. Soc. 108*, 302–303.

Wing, R., Drew, H., Takano, T., Broka, C., Tanaka, S., Itahura, K., & Dickerson, R. E. (1980) *Nature 287*, 755–758.

Wittebort, R. J., Olejniczak, E. T., & Griffin, R. G. (1987) *J. Chem. Phys. 86*, 5411–5420.

Yathindra, N., & Sundaralingam, M. (1973) *Biopolymers 12*, 297–314.